JOURNAL OF APPLIED ELECTROCHEMISTRY 22 (1992) 872–876

Electrodeposition of nickel on vitreous carbon: influence of potential on deposit morphology

E. GÓMEZ*, C. MULLER, W. G. PROUD, E. VALLÉS

Departament de Quimica Fisica, Universitat de Barcelona, Martí i Franqués, 1, 08028 Barcelona, Spain

Received 7 May 1991; revised 11 November 1991

The initial stages of the deposition of nickel on vitreous carbon from aqueous $NiCl_2$ (10^{-2} M adjusted to 1 M in chloride) has been studied using voltammetric and potentiostatic methods. The morphology of the deposits was observed by scanning electron and optical microscopy. A discussion of the relation between the deposition mechanism and the morphology is presented.

1. Introduction

Zinc–nickel alloys are of considerable technological interest as they possess greater corrosion resistance than pure zinc coverings. These alloys are produced by electrodeposition in baths containing mixtures of nickel and zinc salts as well as organic additives. Several mechanisms have been proposed in the literature for the deposition process in different media (sulphate, chloride or Watts bath) and upon different supports [1–6 and references therein]. These mechanisms utilize the presence of an adsorbed nickel compound and/or Ni(I) intermediate. Some workers have related the presence of an Ni(I) intermediate to the appearance of the deposit [5].

In previous work from these laboratories [7] the deposition of nickel on vitreous carbon in chloride medium (1 M in ethanol–water) and the influence of alkylphenol additives was discussed. At a nickel concentration of the order of 10^{-2} M two reduction peaks are observed in the voltammetric curves. The first of these peaks (i.e. that at the more positive potential) was found to be very sensitive to the presence of organic additives. Thus the deposition mechanism is both potential dependant and subject to the effects of adsorbed species.

The objective of the work presented here is to extend this study by analysing electrochemically the deposition process from low concentration Ni(II) solutions centering upon the potential interval corresponding to the two reduction peaks and to relate the results to the appearance and morphology of the deposits. The morphological studies were performed using scanning electron and optical microscopy.

2. Experimental details

The solutions used contained 10^{-2} M $NiCl_2 \cdot 6H_2O$ (Merck analytical grade) and 0.98 M NaCl (Merck analytical grade). All water used was firstly doubly distilled and then treated with a Milipore Milli Q system.

The experiments were carried out in a thermostated three electrode cell (T = 19.5° C). The working and counter electrodes were both Metrohm vitreous carbon rods (2 mm diam.). These electrodes were first polished with alumina of different grades, to a mirror finish, ultrasonically cleaned for 2 min in water and finally rinsed with more water. This treatment was repeated prior to each experiment. In every experiment the connection between the working electrode and the solution was at the solution meniscus only, this was to ensure that the area of the electrode was reproducible without using a resin coated electrode which could introduce problems of contamination.

The reference electrode was a saturated calomel electrode mounted inside a Luggin capillary and all potentials are given with respect to this. All solutions were freshly prepared and deoxygenated with pure argon prior to each experiment.

Electrochemical measurements were made in a conventional three electrode cell using a Belport 105 potentiostat with *iR* compensation, together with an X–Y Philips PM 8133 recorder and a PAR 175 signal generator. The morphology of the deposits was examined with a scanning electron microscope Jeol SM 840 using secondary emission and a Hitachi S-4000 SEM field emission microscope. The optical microscope was a Zeiss Axiovert 405 M.

3. Results

3.1. *Electrochemical study*

The voltammogram corresponding to an aqueous solution of 10^{-2} M $NiCl_2$ in sodium chloride (to 1 M, pH in the range 4.7–4.8) (Fig. 1) shows two reduction peaks (C_1 and C_2, C_1 being a double peak) in the cathodic scan and no appreciable oxidation current in the anodic scan. However, when the scan was reversed at potentials corresponding to the first ascending part of the peak C_1 (Fig. 1), or held for some time at these potentials, an oxidation current is found in the anodic sweep (Fig. 2). Reversing the scan at potentials more negative than the initial part of peak C_1 or if the hold was made at potentials corresponding to the C_2 peak,

* Author to whom all correspondence should be addressed.

0021-891X/92

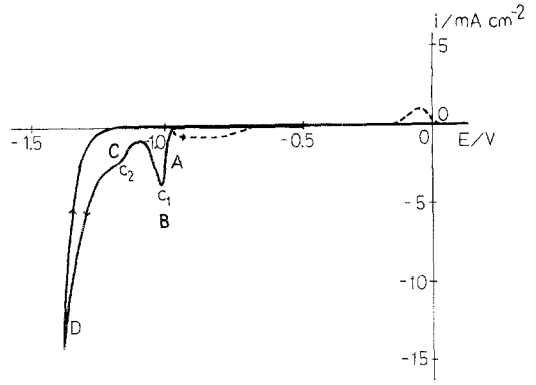

Fig. 1. Cyclic voltammogram of 10^{-2} M $NiCl_2$ and 0.98 M NaCl. $v = 50\,mV\,s^{-1}$. Different limit potentials: (– – –) −970 mV, (——) −1370 mV.

leads to low oxidation currents. This indicates that different kinds of deposits are formed for different potential zones.

The C_1 deposition peak has the characteristics of a nucleation and growth process as a reduction current was observed when the scan as reversed at potentials corresponding to the foot of the peak. Moreover, in the general voltammetric study, it was observed that the C_1 peak was extremely sensitive to the experimental conditions.

The charge corresponding to the C_1 peak was greatly increased with increasing temperature (Fig. 3) and the reduction charge of C_1 also increased with increasing scan rate (Table 1). These facts indicate that the process corresponding to the first peak does not correspond to a simple monolayer formation but to three dimensional growth.

In ethanol–water medium the presence of alkylphenolic compounds supresses the C_1 reduction peak but not the C_2 peak [7]. Similar behaviour was observed in aqueous solutions when hydrogen gas is bubbled into the solution before nickel deposition. It is known [8] that hydrogen gas operates as an inhibitor to nickel deposition and it seems that the initial deposition process is very sensitive to the presence of any kind of inhibitor.

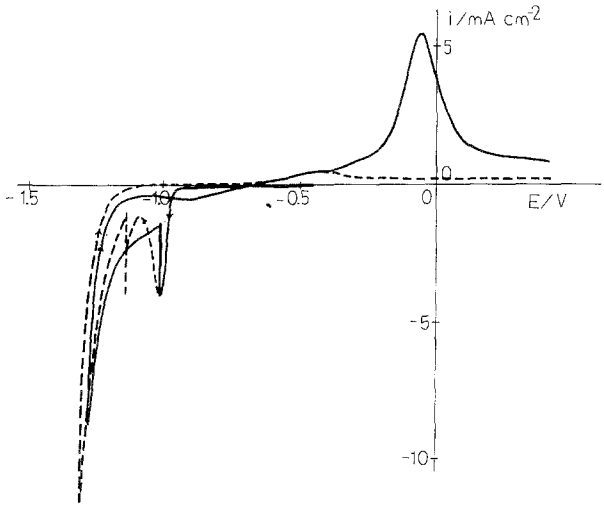

Fig. 2. Influence of potentials during a hold of 30 s in: (——) −1025 mV, (– – –) −1140 mV. $v = 50\,mV\,s^{-1}$.

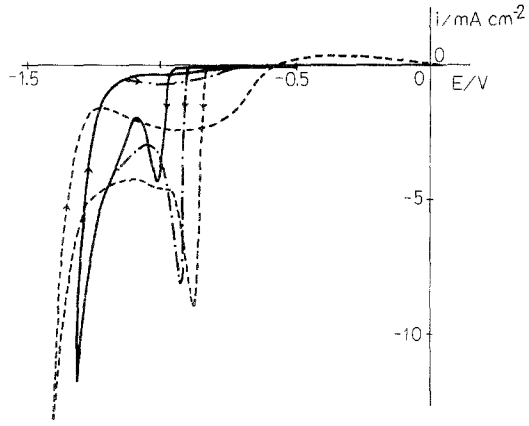

Fig. 3. Cyclic voltammograms at $v = 50\,mV\,s^{-1}$ and different temperatures: (——) 19° C, (–·–·–) 30° C and (– – –) 42° C.

However, modification of solution pH did not qualitatively affect the voltammetric response; only a more negative potential was needed for deposition when the pH was decreased.

This kind of voltammetric curve with two nickel reduction peaks has not been reported previously for a vitreous carbon surface, but a similar curve has been observed for a Pd electrode with weakly acidic chloride solutions [5].

The voltammetric curves allowed various ranges of potential corresponding to reduction peaks C_1 and C_2 to be defined and thus leading to the study of the corresponding potentiostatic curves. The *i–t* curves obtained at different potentials are collected in Fig. 4.

For low cathodic potentials, previous to the C_1 peak or corresponding to the first descending part, an *i–t* curve of the form shown in curve (a) was obtained. The form of the curve was that of a plateau for which, at longer times, the current decayed slowly. When the cathodic potential was further increased a well defined peak followed by a pronounced fall was observed (curve b). Upon analysing these *i–t* curves by means of the model developed by Amstrong *et al.* [9–11] and modified by Barradas and coworkers [12] the curves represented a progressive three dimensional nucleation and growth followed by passivation of electrode at very low cathodic potentials, the passivation parameters increasing with increasing cathodic potential. As is usual at high overpotentials the process becomes an instantaneous three-dimensional nucleation and growth process with passivation.

With increasing overpotential, a new process was detected in potentiostatic curves (curves c–f). At these potentials the *i–t* transients showed an additional peak in the curve, followed by a fall to a stationary current which is a function of the hydrogen evolution on the

Table 1. Comparison of charge corresponding to C_1 peak at different scan rate (v)

$v/mV\,s^{-1}$	$Q/\mu C$
10	320
50	115
100	70

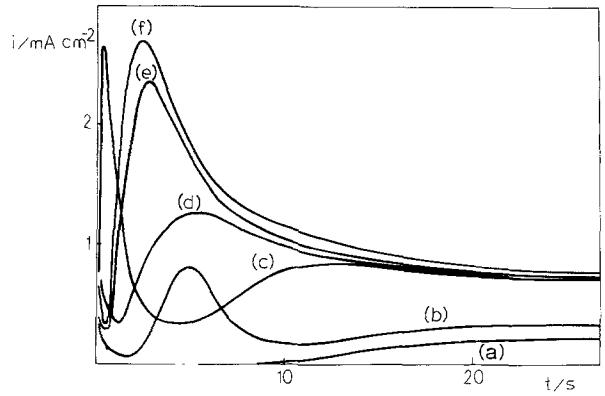

Fig. 4. Potentiostatic transients for Ni deposition for $NiCl_2$ 10^{-2} M and NaCl 0.98 M from $E_0 = -500$ mV to different potentials: (a) −960, (b) −990, (c) −1020, (d) −1100, (e) −1150 and (f) −1175 mV.

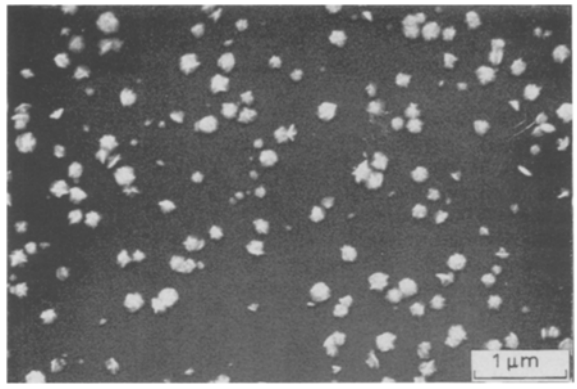

Fig. 5. Scanning electron microscopy for nickel deposition during 45 s at −955 mV.

electrode, which is, in turn, dependant on the applied potential. This second potentiostatic peak suggested that diffusion plays an important role in the control of the process at these potentials. Moreover, the position of this second peak in relation to the first peak, permitted analysis by means of the BFT model [13, 14]. This indicated that the second peak had the characteristics corresponding to a progressive, diffusion controlled, three dimensional growth at relatively low overpotentials.

On the other hand, when hydrogen gas was introduced into the working solution, the *i–t* transient was modified. In comparison with the potentiostatic curves obtained in the absence of hydrogen an induction period was observed. This induction period confirmed that hydrogen operates as an inhibitor and in a similar way to the additives in previous work [7]. When the amount of hydrogen introduced was increased, the inhibition was more pronounced, increasing the induction period.

3.2. *Morphological study*

A morphological study was carried out by means of scanning electron microscopy (SEM) and optical microscopy (OM). This study was made in order to analyse the influence of potential on the first stages of the deposition and to establish the relationship between the deposition potential and the deposit morphology and appearance at high deposition times.

3.2.1. Potentiostatic experiments. The morphology and appearance were studied using deposits obtained by stepping the potential from −0.5 V (potential where no electrode reaction occurs) to more negative values.

Firstly, the shape and size of the first deposited crystals was studied using 45 s of deposition at very low potentials, the deposit consisted of isolated jagged hemispherical nuclei of variable size (Fig. 5) corresponding to a progressive nucleation and growth process. At these potentials 45 s corresponded to the fall in current observed in the *i–t* transient, however, the coalescence of the nuclei had not occured even though the maximum of the curve had been passed. This showed that the maximum in the curve was not related to the coalescence of nuclei but to a passivation process, this is contrary to what occurs in other media [15].

Using a longer deposition time (120 s) and comparing the deposits obtained at various cathodic potentials, it was found that the morphology was, at all potentials, similar. However there was an interval of potentials where inhibition of the deposition process was observed manifested by both smaller number and size of nuclei. When the step was made to even more cathodic potentials, a new increase in the amount of nickel deposited was found and, in this case, 120 s was sufficient to achieve the typical steady current observed in the *i–t* transient (this is referred to in the study of the potentiostatic curves). At potentials for which hydrogen evolution is the dominant reaction (above −1300 mV) only slight Ni deposition is obtained and the crystals have a curious morphology (Fig. 6). These paralepipedical crystals may arise as a consequence of hydrogen adsorption on the nickel deposit thus hindering normal crystal growth.

3.2.2. Voltammetric holds. Scanning electron microscopy was also used to study the morphology of the deposits obtained with a potential hold of 5 min in the different zones of the voltammetric curve, after scanning to the hold potential from −0.5 V (Fig. 7). When an appreciable amount of deposit was found at potentials corresponding to zone A (start of deposition until −1000 mV) (Fig. 7a) it took the form of a compact

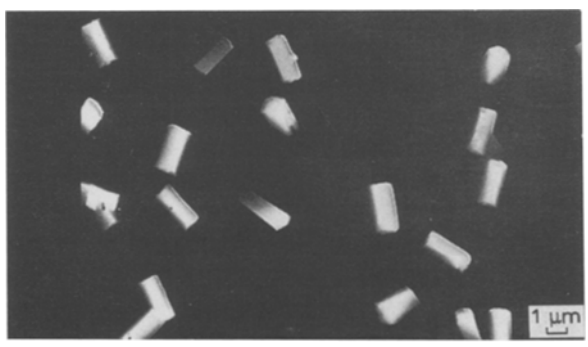

Fig. 6. Scanning electron microscopy for nickel deposition during 250 s at −1300 mV.

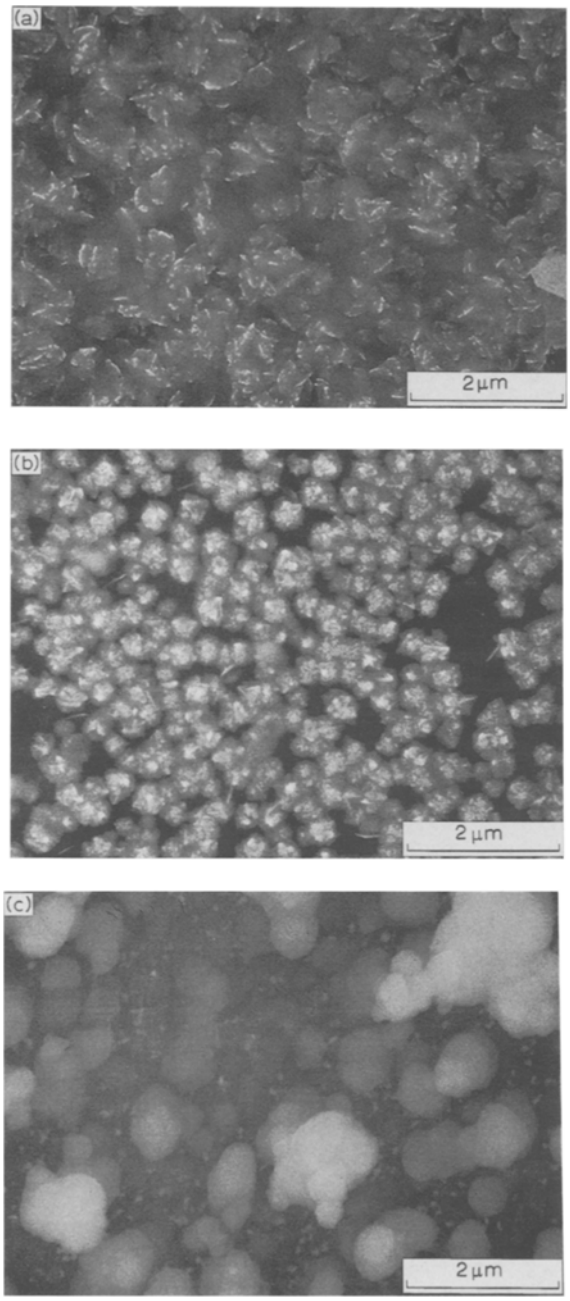

Fig. 7. Scanning electron microscopy for nickel deposition during a hold of 5 min in voltammetry ($v = 50\,mV\,s^{-1}$) at different potential zones defined in Fig. 1: (a) zone A, (b) zone B, and (c) zone C.

deposit of intersecting flakes. For a potential in zone B (from -1000 to $-1060\,mV$) the deposition process was partially inhibited and a covering of aggregates of hemispherical nuclei, of varying size, was obtained without any indication of an underlying, or first, layer (Fig. 7b). At potentials corresponding to zone C abundant deposition was obtained (Fig. 7c) whereas at potentials even more negative only a few crystals were observed, corresponding to the dominance of the evolution of hydrogen gas observed during the hold (zone D).

In order to obtain information on the macroscopic appearance of the deposits, nickel deposits were obtained using a potential hold of 15 min.

When the hold was made in zone A of peak C_1 an adherent semi-dull black deposit was obtained, which

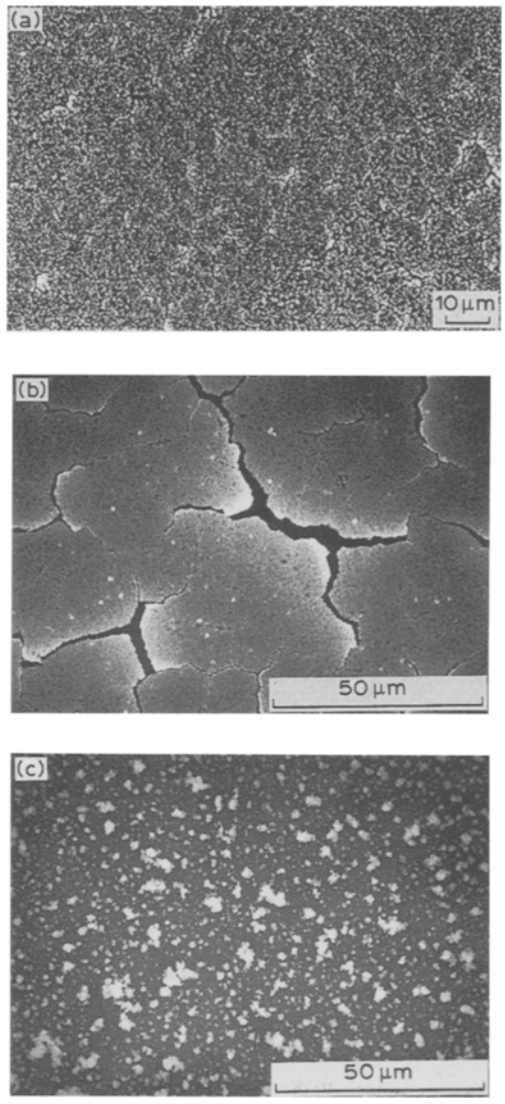

Fig. 8. Scanning electron microscopy for nickel deposition during a hold of 15 min in voltammetry ($v = 50\,mV\,s^{-1}$) at different potential zones: (a) zone A, (b) zone B and (c) zone C.

corresponds to a compact deposit (Fig. 8a). At potentials corresponding to zone B a brighter nickel deposit was obtained which had a very low adherence to the electrode; the deposit cracked and detached itself very easily from the electrode (Fig. 8b).

The deposit obtained at potentials corresponding to C_2 peak, was an adherent clear grey deposit with a granular structure (Fig. 8c).

4. Discussion

The differing morphologies of the deposits may be related to the relative predominance of steps in the deposition at different potentials as has been stated previously by other authors. In particular Ragauskas and Leuksminas [5] have reported, for nickel deposition on palladium electrode in chloride media, voltammetric curves similar to those reported here. These authors obtain deposits of differing characteristics depending upon the position of the deposition potential in relation to the peak observed in the polarization curve.

In the mechanisms proposed for nickel deposition

one of the first steps [4, 5, 16] is the reduction of Ni(II)

$$Ni(II) + 1e^- \longrightarrow Ni(I) \quad (1)$$

followed by either one or more steps that lead deposition. This simple scheme may correspond to potentials in zone A, and may explain the compact, uniform deposits obtained.

On the other hand, the different and scarcely adherent deposits obtained in zone B suggest a change in the overall process. At these potentials the first step is maintained but is followed by a possible disproportion reaction of Ni(I); disproportionation is commonly observed for monovalent ions of elements of higher valency and generates deposits with a high level of dispersion.

$$Ni(I) + Ni(I) \longrightarrow Ni(O) + Ni(II) \quad (2)$$

Moreover, simultaneously in these conditions the reaction between Ni(I) and H_2O

$$Ni(I) + H_2O \longrightarrow NiOH(I) + H \quad (3)$$

may occur. Reaction 3 explains the simultaneous production of hydrogen during the nickel deposition.

It has been reported [5] that in the potential zone in which disproportion is predominant, significant hydrogen evolution is detected. In zone B hydrogen evolution is not dominant but could be responsible for the low adherence of the deposit. Moreover, an inhibition of the process takes place indicated by the relative reduction of both the size and number of crystals compared to deposits obtained in zone A. This fact is verified by both scanning electron and optical microscopy and corresponds to the inhibition observed at intermediate potentials in the potential step experiments. The final deposit, cracked, disperse and fined grained could be the consequence of both the disproportion of Ni(I) and hydrogen evolution. The existence of secondary reactions in zone B is probably responsible for the lower quantity of nickel deposited for the same deposition time. Moreover, the disproportion step modifies the appearance of the deposit, leading to a more disperse structure. Simultaneous hydrogen evolution aids cracking of the deposit and a fine grained deposit is produced if hydrogen is adsorbed on the nickel layer thus impeding growth of the nuclei.

When deposition is performed at more negative potentials (zone C) a compact and uncracked deposit is again obtained. At these potentials the dominant reaction path is that which leads to nickel deposition – the side reactions of type Reaction 3 being of reduced importance – giving a compact deposit. At more negative potentials, hydrogen evolution on the vitreous carbon electrode is the predominant reaction and very little nickel deposition is obtained in zone D.

Acknowledgements

The authors are grateful for financial assistance to the Comisión de Investigación Científica y Técnica (Project number PB87–0593) and to the Serveis Cientifico–Tecnics of the Universitat de Barcelona.

References

[1] I. Epelboin and R. Wiart, *J. Electrochem. Soc.* **118** (1971) 1577.
[2] I. Epelboin, M. Joussellin and R. Wiart, *J. Electroanal. Chem.* **119** (1981) 61.
[3] E. Chassaing, M. Joussellin and R. Wiart, *ibid.* **157** (1983) 75.
[4] A. Saraby-Reintjes and M. Fleischmann, *Electrochim. Acta* **29** (1984) 557.
[5] R. Ragauskas and V. Leuksminas, *Sov. Electrochem.* **24** (1988) 675.
[6] Chr. Bozhkov, Chr. Tzvetkova and St. Rashkov, *J. Electroanal. Chem.* **296** (1990) 453.
[7] R. Albalat, E. Gomez, C. Muller, M. Sarret and E. Vallés, *J. Appl. Electrochem.* **21** (1991) 709–15.
[8] C. Kollia, N. Spyrellis, J. Amblard, M. Froment and G. Maurin, *J. Appl. Electrochem.* **20** (1990) 1025.
[9] R. D. Armstrong, M. Fleischmann and H. R. Thirsk, *J. Electroanal. Chem.* **11** (1966) 208.
[10] M. Fleischmann and H. R. Thirsk, 'Advances in Electrochemistry and Electrochemical Engineering', Vol. 3 (edited by P. Delahay), Wiley & Sons, New York (1963).
[11] J. A. Harrison and H. R. Thirsk, 'Electroanalytical Chemistry', Vol. 5 (edited by A. J. Bard), Academic Press, New York (1971).
[12] R. G. Barradas, F. C. Benson and S. Fletcher, *J. Electroanal. Chem.* **80** (1977) 305.
[13] A. Bewick, M. Fleischmann and H. R. Thirsk, *Trans. Faraday Soc.* **58** (1962) 2200.
[14] J. A. Harrison and H. R. Thirsk, in 'Electroanalytical Chemistry', Vol. 5 (edited by A. J. Bard), Marcel Dekker, New York (1971) p. 67.
[15] J. Amblard, M. Froment, G. Maurin, D. Mercier and E. Trevisan-Pikacz, *J. Electroanal. Chem.* **134** (1982) 345.
[16] Chr. Bozhkov and St. Rashkov, *B. Electrochem.* **5** (1989) 756.